The KCNQ5 potassium channel mediates a component of the afterhyperpolarization current in mouse hippocampus

Anastassios V. Tzingounis[a,1,2], Matthias Heidenreich[b,1], Tatjana Kharkovets[c], Guillermo Spitzmaul[b], Henrik S. Jensen[d,3], Roger A. Nicoll[a,4], and Thomas J. Jentsch[b,c,4]

[a]Department of Cellular and Molecular Pharmacology and Department of Physiology, University of California, San Francisco, CA 94143; [b]Leibniz-Institut für Molekulare Pharmakologie (FMP) and Max-Delbrück-Centrum für Molekulare Medizin (MDC), Berlin, D-13125, Germany; [c]Zentrum für Molekulare Neurobiologie (ZMNH), Universität Hamburg, Hamburg, D-20251, Germany; and [d]Department of Medical Physiology, The Panum Institute, University of Copenhagen, Copenhagen, DK-2200, Denmark

Contributed by Roger A. Nicoll, April 8, 2010 (sent for review February 18, 2010)

Mutations in KCNQ2 and KCNQ3 voltage-gated potassium channels lead to neonatal epilepsy as a consequence of their key role in regulating neuronal excitability. Previous studies in the brain have focused primarily on these KCNQ family members, which contribute to M-currents and afterhyperpolarization conductances in multiple brain areas. In contrast, the function of KCNQ5 (Kv7.5), which also displays widespread expression in the brain, is entirely unknown. Here, we developed mice that carry a dominant negative mutation in the KCNQ5 pore to probe whether it has a similar function as other KCNQ channels. This mutation renders KCNQ5^{dn}-containing homomeric and heteromeric channels nonfunctional. We find that *Kcnq5*$^{dn/dn}$ mice are viable and have normal brain morphology. Furthermore, expression and neuronal localization of KCNQ2 and KCNQ3 subunits are unchanged. However, in the CA3 area of hippocampus, a region that highly expresses KCNQ5 channels, the medium and slow afterhyperpolarization currents are significantly reduced. In contrast, neither current is affected in the CA1 area of the hippocampus, a region with low KCNQ5 expression. Our results demonstrate that KCNQ5 channels contribute to the afterhyperpolarization currents in hippocampus in a cell type-specific manner.

M-current | sAHP | calcium | epilepsy | KCNQ

A train of action potentials can be terminated through the opening of multiple potassium channels activated by depolarized voltages, incoming calcium, or both (1, 2). A slow calcium-activated potassium conductance plays a prominent role in the cessation of neuronal firing in most pyramidal neurons (3). This potassium conductance is highly regulated by various neurotransmitters and neuromodulators and has been implicated in sleep-wake cycles (4), synchronized burst activity in neuronal populations (5), long-term potentiation (6), and learning and memory (7, 8). Recently, we have proposed that the calcium activation of this potassium slow afterhyperpolarization (sAHP) current is through hippocalcin (9), a diffusible neuronal calcium sensor (NCS) that translocates to the membrane after binding cytosolic calcium (10). As a result, the sAHP current reports global cytosolic calcium changes instead of only calcium fluctuations close to the membrane. Despite sAHP's significant contribution to regulating neuronal excitability and unique gating mechanism, the potassium channels mediating this current remain elusive (11). A possible breakthrough has come with the observation that genetically induced loss of KCNQ2 or KCNQ3 function impairs the sAHP current in a cell type-specific manner (12). This has raised the unexpected possibility that KCNQ channels, known mediators of the M-current (13) and principal contributors to medium afterhyperpolarization (mAHP) (2, 14), might have a dual role in hippocampus.

In addition to KCNQ2 and KCNQ3, KCNQ5 is widely distributed in the brain, including the hippocampus (15–17). In contrast, KCNQ4 is found only in a few nuclei and tracts mainly in the brainstem (18). Unlike KCNQ2 and KCNQ3, the function of KCNQ5 in the brain remains unknown and no neurological disorders have been attributed to it. Given KCNQ5's similar biophysical properties to other members of the KCNQ family, KCNQ5 may also contribute to M-currents (15, 16). To elucidate the physiological functions of KCNQ5 and test whether KCNQ5 also has a role in AHP currents, we generated knock-in (KI) mice carrying a dominant negative (dn) mutation in KCNQ5. In *Kcnq5*$^{dn/dn}$ mice, channels containing at least one KCNQ5 subunit are expected to be nonfunctional, including KCNQ3/KCNQ5 heterooligomers that normally yield higher currents than KCNQ5 homooligomers (15, 16). By contrast, the KO of *Kcnq5* may paradoxically increase M-currents in cells also expressing KCNQ2 and KCNQ3 because KCNQ3 subunits that normally associate with KCNQ5 may now be free to assemble into more efficient KCNQ2/KCNQ3 heteromers.

Using these mice, we show here that KCNQ5 contributes to the mAHP and sAHP currents (ImAHP and IsAHP) in CA3 pyramidal neurons of the hippocampus. Our data present a demonstration of a KCNQ5 function in the brain and further support the role of molecularly diverse KCNQ channels in mediating AHP current components.

Results

Dominant Negative KCNQ5 KI Mice. To investigate the physiological roles of the KCNQ5 channel, we created a KI mouse carrying a dominant negative mutation in KCNQ5. We mutated the first glycine of the GYG signature pore sequence of KCNQ5 to serine (G278S). Equivalent human mutations have been found in KCNQ1 with the dominant form of the long QT syndrome (19) and in KCNQ4 in a family with dominant deafness (20). These mutations, as well as equivalent mutations introduced into KCNQ2 and KCNQ3, were shown to have dominant negative effects in heterologous expression (15, 20, 21). KCNQ3 can form functional heteromers with KCNQ5 (15, 16). On heterologous expression in *Xenopus* oocytes, KCNQ3 induces currents that are barely above background. Coexpression of KCNQ3 with KCNQ5 boosts currents in oocytes more than 2-

Author contributions: A.V.T., R.A.N., and T.J.J. designed research; A.V.T., M.H., T.K., G.S., and H.S.J. performed research; A.V.T., M.H., and G.S. analyzed data; and A.V.T., M.H., G.S., R.A.N., and T.J.J. wrote the paper.

The authors declare no conflict of interest.

[1]These authors contributed equally to this work.

[2]Present address: Department of Physiology and Neurobiology, University of Connecticut, Storrs, CT 06269.

[3]Present address: H. Lundbeck A/S, Department of Molecular Neurobiology, Copenhagen, DK 2500, Denmark.

[4]To whom correspondence may be addressed. E-mail: nicoll@cmp.ucsf.edu or jentsch@fmp-berlin.de.

This article contains supporting information online at www.pnas.org/lookup/suppl/doi:10.1073/pnas.1004644107/-/DCSupplemental.

fold with respect to KCNQ5 homooligomers (15). Dominant negative effects of KCNQ3(G318S) on KCNQ5 currents have been demonstrated before (15). We now tested whether KCNQ5(G278S), which is nonfunctional by itself (15), exerts dominant negative effects on KCNQ5 and on KCNQ3/KCNQ5 heteromers (an effect on KCNQ3 homomers cannot be tested because of low currents). As described before (15), currents increased more than 2-fold with respect to KCNQ5 homomers when KCNQ3 and KCNQ5 were coinjected at a 1:3 ratio (Fig. 1 *A* and *B*). Coinjection of KCNQ5 WT with G278S mutant (1:1) decreased KCNQ5 current more than 90%, demonstrating the strong dominant negative effect of the mutant subunit. Oocytes injected with KCNQ3, KCNQ5, and KCNQ5 (G278S) in a 1:1.5:1.5 ratio exhibited a small current of about 15% of KCNQ3/KCNQ5 (1:3) current (Fig. 1 *A* and *B*), indicating that KCNQ5(G278S) also exerts a dominant negative effect on KCNQ3/KCNQ5 heteromers. Currents were indistinguishable from background when KCNQ3 was coexpressed with KCNQ5(G278S) (Fig. 1 *A* and *B*), a situation that may arise in homozygous KI mice.

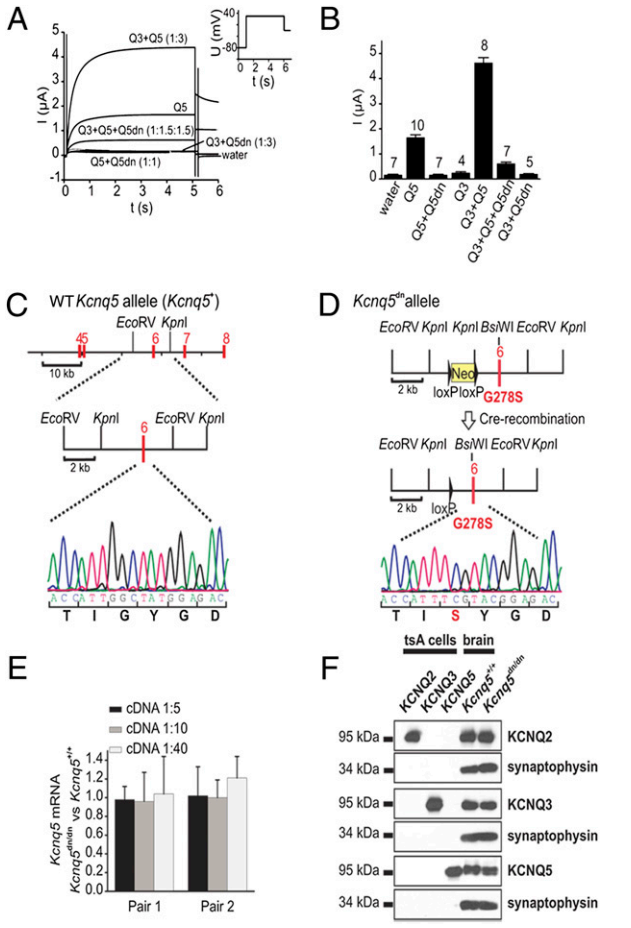

Fig. 1. Generation of dominant negative *Kcnq5* KI mice. (*A*) Effect of KCNQ5(G278S) on currents elicited by KCNQ5 homomers and KCNQ3/KCNQ5 heteromers. Oocytes were injected with the same total amount of RNA with the indicated concentration ratios. t, time. (*Inset*) Oocytes were clamped for 5 s to +40 mV. (*B*) Averaged currents (at +40 mV) from oocytes injected with the indicated combinations of KCNQ3, KCNQ5, and KCNQ5(G278S) RNAs. Error bars, SEM. Number of oocytes (from three or more different batches) is indicated above columns. Scheme of mouse genomic WT *Kcnq5* sequence (*C*) and mouse genomic dominant-negative *Kcnq5* sequence (*D*). A NEO selection cassette flanked by loxP sites was introduced into intron 5, together with three point mutations in exon 6 that replace glycine 278 by serine and additionally generate a BsiWI restriction site. The NEO cassette was removed by Cre-recombinase in vitro (exons shown in red). (*E*) Quantitative real-time RT-PCR analysis of *Kcnq5(G278S)* mRNA expression in brain, normalized to *Kcnq5* mRNA found in WT brain. (*F*) Western analysis of whole-brain membrane preparations (P65) of KCNQ2, KCNQ3, and KCNQ5 from $Kcnq5^{+/+}$ and $Kcnq5^{dn/dn}$ mice. Lysates of transfected tsA cells were used as controls for antibody specificity. $Kcnq5^{dn/dn}$ mice have normal expression levels of KCNQ2, KCNQ3, and KCNQ5.

Having verified the dominant negative effects of the KCNQ5 (G278S) mutant, we introduced this mutation into the murine *Kcnq5* gene by homologous recombination in ES cells. For genotyping purposes, we also inserted a *Bsi*WI restriction site (Fig. 1 *C* and *D*). These alterations required the mutation of a total of 4 base pairs. A neomycin (NEO) cassette flanked by loxP sites was inserted into intron 5 for selection. It was later removed by treating ES cells with Cre-recombinase (Fig. 1*D*). This allele is called $Kcnq5^{dn}$. $Kcnq5^{dn/dn}$ mice were derived from targeted ES cells. Sequencing of genomic DNA from these mice confirmed the changes in the pore domain (Fig. 1*D*) and the presence of one remaining loxP site.

We next compared KCNQ5 mRNA and protein levels between $Kcnq5^{dn/dn}$ and WT mice. Using quantitative RT-PCR of RNA extracted from total brain, we found no significant differences between WT and $Kcnq5^{dn/dn}$ mice (Fig. 1*E*). Similarly, Western blot analysis did not reveal any differences in the expression of the KCNQ5 protein levels in whole brain between WT and $Kcnq5^{dn/dn}$ mice (Fig. 1*F*). Importantly, the expression of KCNQ2 and KCNQ3 was unchanged in $Kcnq5^{dn/dn}$ mice (Fig. 1*F* and Fig. S1), suggesting that there is no compensatory up-regulation of those other major KCNQ isoforms in $Kcnq5^{dn/dn}$ brain. Moreover, the subcellular localization of KCNQ2 and KCNQ3 subunits to axon initial segments of hippocampal pyramidal cells was not changed (Fig. 2*A*).

Mice carrying the dominant negative allele were born at a less than Mendelian ratio. Among 147 pups resulting from crossing $Kcnq5^{+/dn}$ mice, we observed 41.4% $Kcnq5^{+/+}$, 46.2% $Kcnq5^{+/dn}$, and 12.4% $Kcnq5^{dn/dn}$ animals. However, $Kcnq5^{dn/dn}$ mice displayed normal postnatal development and lifespan and lacked visible phenotypes. The morphology of the brains of $Kcnq5^{dn/dn}$ mice is grossly normal, as revealed by histological analysis at two different ages, postnatal day (PD) 65 (Fig. 2*B*) and PD 18 (Fig. S2), in regions of high *Kcnq5* expression (15), such as the hippocampus and cortex, or in regions of low expression, such as the cerebellum (Fig. 3*A*).

Effect of KCNQ5 Dominant Negative Mutation on the ImAHP and IsAHP in the Hippocampus. We first examined the distribution of KCNQ5 and KCNQ3 within the brain, particularly within the hippocampus, using immunohistochemistry. KCNQ5 was found to be prominently expressed in the hippocampus, where the highest levels were visible in the CA3 region (Fig. 3 *A* and *B*). CA1 and CA2 pyramidal cells as well as dentate gyrus granule cells showed weaker KCNQ5 expression than those in the CA3 region (Fig. 3*B*). Similar to KCNQ5, KCNQ3 protein showed robust expression in the hippocampus, most prominently in the subiculum, mossy fibers, and CA1 and CA2 pyramidal cells (Fig. 3 *C* and *D*). This expression pattern of KCNQ3 and KCNQ5 protein agrees with previous published mRNA data (15, 21) and with data from the Allen brain atlas (22).

To determine the relative contribution of KCNQ5 to the mAHP and sAHP currents, we compared the ImAHP and IsAHP recorded from WT and $Kcnq5^{dn/dn}$ mice. We decided to focus on CA1 and CA3 pyramidal neurons in the hippocampus because they both express KCNQ5 and KCNQ3 but at different expression levels, as shown above. In slices from WT mice and in the presence of 100 nM apamin to block SK channels, a 100-ms depolarizing pulse from −55 mV to +25 mV in CA1 or CA3 pyramidal neurons robustly elicits the ImAHP and IsAHP. We found that in CA1 neurons, the apamin-insensitive mAHP current is unaffected in $Kcnq5^{dn/dn}$ mice, but it is decreased by almost 50% in CA3 pyramidal neurons (Fig. 4 *A* and *B*). Specifically, the ImAHP amplitude in WT CA1 pyramidal neurons is 293 ± 17 pA (n = 15 cells from six WT mice), whereas in $Kcnq5^{dn/dn}$ mice, it is 250 ± 36 pA (n = 16

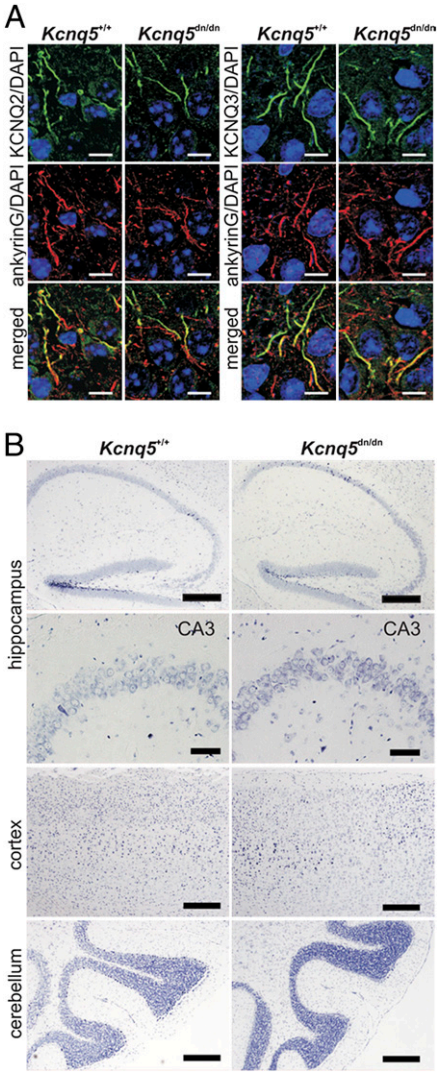

Fig. 2. Normal subcellular localization of KCNQ2 and KCNQ3 and unchanged brain histomorphology in *Kcnq5*$^{dn/dn}$ mice. (*A*) KCNQ2 and KCNQ3 are localized to ankyrinG-positive axon initial segments in hippocampus pyramidal cells in both *Kcnq5*$^{+/+}$ and *Kcnq5*$^{dn/dn}$ mice. (*B*) Nissl staining of sagittal sections of the hippocampus, cortex, and cerebellum shows normal histomorphology in *Kcnq5*$^{dn/dn}$ mice at PD65. Higher magnification of the CA3 area is shown. (Scale bars: *A*, 10 μm; *B*, 500 μm; higher magnification of CA3, 100 μm.)

cells from four *Kcnq5*$^{dn/dn}$ mice; $P = 0.30$, Student's t test). In contrast, in CA3 pyramidal neurons, the ImAHP amplitude is 201 ± 28 ($n = 21$ cells from six WT mice) and 107 ± 19 pA ($n = 13$ cells from three *Kcnq5*$^{dn/dn}$ mice; $P < 0.05$, Student's t test) in WT and *Kcnq5*$^{dn/dn}$ mice, respectively. Additionally, the sensitivity of the apamin-insensitive ImAHP to 10 μM XE991, a specific M-current and KCNQ2/KCNQ3 blocker, is similar between WT and *Kcnq5*$^{dn/dn}$ mice (WT: $54 \pm 13\%$, $n = 4$ from two mice; *Kcnq5*$^{dn/dn}$: $55 \pm 3\%$, $n = 3$ from one mouse; $P = 0.95$). We also did not see any changes in the input resistance (WT: 180 ± 10 MΩ, $n = 21$ from six mice; *Kcnq5*$^{dn/dn}$: 194 ± 18 MΩ, $n = 14$ from three mice; $P = 0.47$, Student's t test) or in the apamin-sensitive ImAHP (I-SK) in mice carrying the *Kcnq5*^{dn} gene (I-SK WT: 162 ± 14 pA, $n = 8$ from four mice; I-SK *Kcnq5*^{dn}: 130 ± 18 pA, $n = 7$ from three mice; pooled data from *Kcnq5*$^{dn/dn}$ and *Kcnq5*$^{+/dn}$ mice; $P = 0.1786$, Student's t test). These data then suggest that KCNQ5 can contribute to the ImAHP CA3 but not CA1 neurons of the hippocampus.

To quantify the role of KCNQ5 in the sAHP current, we measured both the charge transfer (QsAHP) and the amplitude of the IsAHP in CA1 and CA3 pyramidal neurons of WT and *Kcnq5*$^{dn/dn}$ mice. As shown in Fig. 4 *C* and *D*, the QsAHP and IsAHP amplitude from *Kcnq5*$^{dn/dn}$ mice recorded from CA1 pyramidal neurons is similar to the responses recorded in WT mice (IsAHP WT: 39 ± 4 pA, $n = 15$ cells from six mice; *Kcnq5*$^{dn/dn}$: 40 ± 5 pA, $n = 16$ cells from four mice; $P = 0.86$, Student's t test). In contrast, the QsAHP was significantly decreased by about 25–30% in CA3 pyramidal neurons from *Kcnq5*$^{dn/dn}$ mice (QsAHP WT: 2155 ± 149 pC, $n = 21$ cells from six mice; *Kcnq5*$^{dn/dn}$: 1524 ± 110 pC, $n = 14$ cells from three mice; $P < 0.005$, Student's t test). As with the QsAHP (Fig. 4*D*), the IsAHP amplitude is decreased to similar levels in CA3 pyramidal neurons (IsAHP WT: 457 ± 30 pA, $n = 21$ cells from six mice; *Kcnq5*$^{dn/dn}$: 342 ± 26, $n = 14$ from three mice; $P = 0.05$, Student's t test). We also measured the WT IsAHP in the presence of 10 mM 1,2-bis (2-aminophenoxy) ethane-N,N,N′,N′-tetraacetic acid (BAPTA) to ensure that the current we are referring to as the IsAHP in CA3 neurons is attributable to the calcium-activated sAHP. In WT cells in which BAPTA was included in the pipette, the IsAHP is 23 ± 3 pA ($n = 4$ from one mouse) as opposed to the IsAHP in the absence of BAPTA, which is 457 ± 30 pA ($n = 21$ from six WT mice). Together, these data indicate that the IsAHP and ImAHP recorded in CA3 pyramidal neurons are partly mediated by KCNQ5 homomers or KCNQ3/5 heteromers. Currently, we cannot distinguish between these two possibilities.

Discussion

KCNQ channels have been implicated in mediating AHP conductances in neurons, but the contribution of individual KCNQ channel family members to the mAHP current has remained unknown because of the lack of subtype-selective KCNQ channel blockers. An added complicating factor is that KCNQ channels can form homomers as well as heteromers with each other (i.e., KCNQ2/KCNQ3, KCNQ3/KCNQ5, KCNQ3/KCNQ4), thus creating multiple possible combinations of KCNQ-mediated currents (23, 24). KCNQ5 is the final member of the KCNQ family without a known biological role. To elucidate its contribution to AHP currents, we used mice expressing dominant negative KCNQ5 channels [KCNQ5(G278S)] driven by their native promoter, allowing us to bypass the need for specific KCNQ5 blockers. These mice provide evidence that KCNQ5 contributes to the mAHP and sAHP currents in a cell type-selective manner.

KCNQ5 and the ImAHP. Several studies have supported the notion that KCNQ2 and KCNQ3 are major contributors to the apamin-insensitive component of ImAHP (14, 24, 25). We have found that KCNQ5 is highly expressed in CA3 and contributes to ImAHP in CA3 pyramidal neurons, thus extending the number of KCNQ family members known to contribute to mAHP. In contrast, KCNQ5(G278S) had no effect on ImAHP in CA1 neurons. This cell type-specific contribution is most likely attributable to the differential expression of KCNQ2, KCNQ3, and KCNQ5 protein in the hippocampus. In particular, we showed that KCNQ5 protein is sparse in CA1 compared with CA3, which is consistent with the *Kcnq5* mRNA level in the hippocampus (22, 26). Our results are consistent with our previous finding that KCNQ3 KO and KCNQ2 heterozygous mice have significantly reduced mAHP currents in dentate granule cells, neurons that have high mRNA and protein levels for both of these subunits, but that KCNQ5 mice do not. In contrast, the situation in CA1 pyramidal neurons appears more complicated. Like CA3 pyramidal neurons, CA1 pyramidal neurons express all three KCNQ subunits, but the mAHP current was unaffected in the *Kcnq5*$^{dn/dn}$, *Kcnq2*$^{+/-}$ heterozygous, and *Kcnq3*$^{-/-}$ mice. Others have found that mice overexpressing dominant negative KCNQ2 from a broadly active promoter have significantly diminished mAHP in CA1 pyramidal neurons (14). In the latter mouse model, both KCNQ2 and KCNQ3 currents should be re-

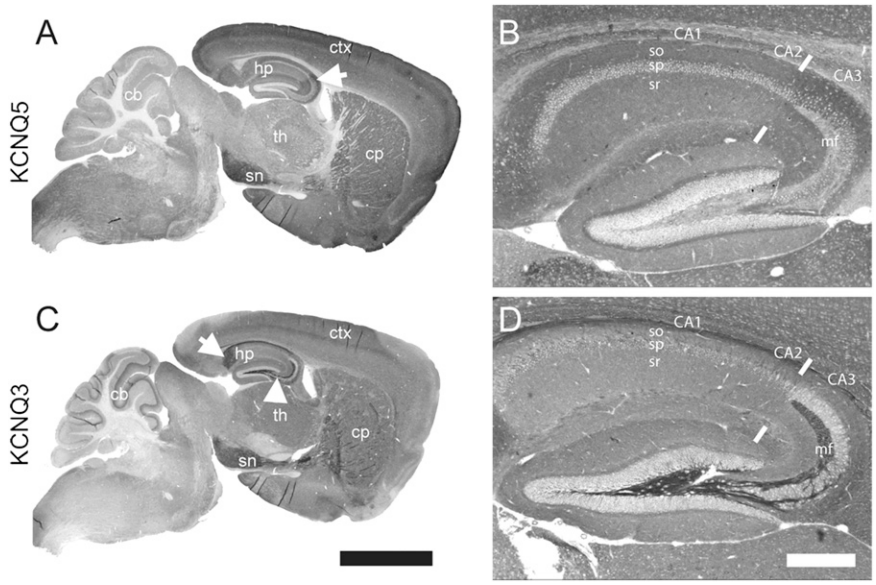

Fig. 3. Expression of KCNQ3 and KCNQ5 proteins in adult brain. (*A*) Immunohistochemistry revealed strong expression of KCNQ5 in the CA3 region of the hippocampus (arrow) and in the cortex, caudoputamen, and substantia nigra but weak expression in the thalamus and cerebellum. (*B*) Higher levels of KCNQ5 in hippocampal CA3 pyramidal cells in contrast to lower levels in CA1 and CA2 pyramidal cells and mossy fibers are shown. (*C*) Strong expression of KCNQ3 was found in the subiculum (arrow) and mossy fibers (arrowhead) of the hippocampus and in the cortex, caudoputamen, substantia nigra, and thalamus. (*D*) Higher levels of KCNQ3 in hippocampal CA1 and CA2 pyramidal cells and mossy fibers in contrast to lower levels in CA3 pyramidal cells are shown. cb, cerebellum; cp, caudoputamen; ctx, cortex; hp, hippocampus; mf, mossy fibers; sn, substantia nigra; so, stratum oriens; sp, stratum pyramidale; sr, stratum radiatum; th, thalamus. The CA2/CA3 border is indicated by white bars in *B* and *D*. (Scale bars: *A* and *C*, 0.25 cm; *B* and *D*, 500 μm.)

pressed. The possibility that KCNQ2 is the predominant contributor to the mAHP current in these neurons could be tested by using KCNQ2 conditional KO mice to avoid the lethal phenotype of the conventional KCNQ2 KO mice (27).

KCNQ5 and the IsAHP. Unlike the ImAHP, the contribution of KCNQ channels to the IsAHP is controversial. KCNQ channels have properties that are both similar to and different from those of the sAHP current. Both KCNQ channels and sAHP have slow activation kinetics that are temperature-sensitive [IsAHP Q_{10}: 3–4 (28); KCNQ2, KCNQ3 Q_{10}: 3–4 (29)]. They also share a small single-channel conductance [IsAHP: 2–8 pS (28, 30), KCNQ5: 2–3 pS; KCNQ2/KCNQ3: 8–10 pS (31–33)], have a probability of opening comparable to that of the sAHP current (28, 31), and are sensitive to modulation by muscarinic and glutamatergic metabotropic receptors (1, 24, 34). However, the IsAHP is thought to be a voltage-independent process, whereas KCNQ channels are voltage-activated (3, 24). Additionally, protein kinase A (PKA) activation blocks the IsAHP (35), whereas PKA activation facilitates KCNQ channels in a subunit-specific manner (21). These differences may be attributable to the calcium activation mechanism of the IsAHP. We have recently shown that the NCS hippocalcin is a key component in the activation of the IsAHP and that it may partially account for the PKA sensitivity of the IsAHP (9).

Currently, the evidence that KCNQ channels also mediate sAHP consists of limited pharmacological and genetic data. Application of either XE991 or linopirdine has been reported to inhibit the IsAHP partially in some studies (12, 36), but this finding has not been reproduced by all groups (25, 37). Recently, we demonstrated that KCNQ2- and KCNQ3-deficient mice have a reduced IsAHP in some types of hippocampal neurons (12). Here, we report that the IsAHP in CA3 pyramidal cells from *Kcnq5*$^{dn/dn}$ mice is impaired, supporting the possibility that KCNQ channels participate in the generation of the IsAHP. Like the ImAHP, the IsAHP may be mediated by different KCNQ family members in different neurons. Here, we find evidence that KCNQ5 may contribute to the IsAHP in CA3 but not CA1 pyramidal neurons, correlating with the high expression levels in CA3. Conversely, our previous study found that KCNQ3 and KCNQ2 are likely to contribute to the IsAHP in dentate granule cells. These cells prominently express KCNQ3, as is evident from the strong staining of mossy fibers that represent axons of those cells (Fig. 3*B*). Could the changes seen in the ImAHP amplitude in KCNQ-deficient mice lead to an apparent decrease in the sAHP current? We think this is unlikely because the kinetics of the mAHP currents are much faster than the rise and decay kinetics of the IsAHP, thus making little contribution to the IsAHP. Additionally, application of apamin to the ImAHP to block SK responses does not affect the sAHP current (9), consistent with the notion that changes to the ImAHP do not translate to a decrease in the IsAHP.

If KCNQ channels mediate both the ImAHP and IsAHP, the mechanism by which KCNQs mediate two temporally distinct conductances is intriguing. We tentatively propose that the ImAHP primarily reflects voltage-dependent activation and deactivation of KCNQ channels, whereas the IsAHP reflects delayed activation of KCNQ channels as a result of dependence on NCS activity. Recently, Tzingounis et al. (9) have shown that the diffusable NCS protein hippocalcin is involved in activating sAHP currents in the brain. The participation of the NCSs imposes a short time delay on the activation of sAHP because the NCSs must first bind cytosolic calcium and translocate to the membrane before gating sAHP current. Consequently, this will give rise to a delay between the ImAHP and IsAHP time course. However, the mechanism by which the NCSs activate the IsAHP is unknown. We speculate that NCS activation may occur through either (*i*) the direct binding of NCSs to KCNQ channels or (*ii*) relief of tonic kinase inhibition of KCNQ channels. Several groups have previously shown that the sAHP channels are under tonic inhibition by various kinases, including PKA and MAPK (38–40), and it is possible that NCS proteins induce a signal transduction cascade leading to removal of tonic kinase activity. Further experiments are needed to explore these possibilities.

The search for the components of sAHP is currently at a crossroads. It has been over 20 years since the first description of sAHP (41, 42), but a molecular description of the channel and its calcium-sensitive gating mechanism has remained elusive (11). Together,

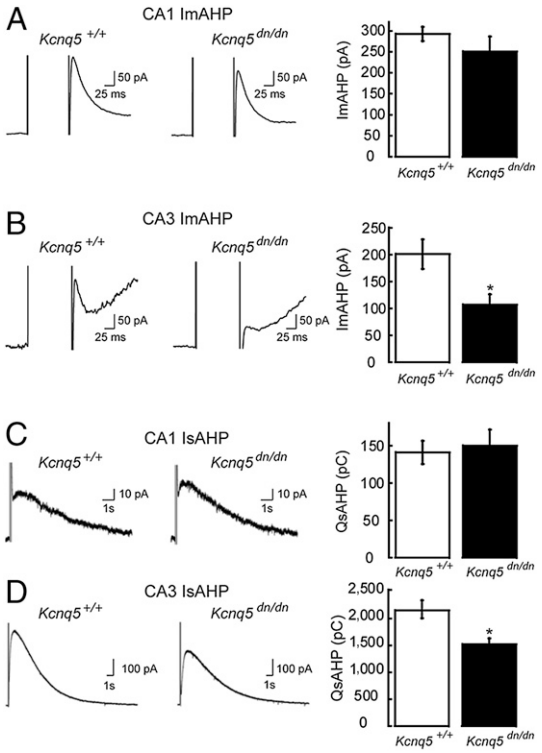

Fig. 4. Loss of the IsAHP and ImAHP in *Kcnq5*$^{dn/dn}$ mice is cell type-specific. (*A*) (*Left* and *Center*) ImAHP in either *Kcnq5*$^{+/+}$ or *Kcnq5*$^{dn/dn}$ mice recorded from CA1 pyramidal neurons. (*Right*) Summary graph of the ImAHP amplitude in *Kcnq5*$^{+/+}$ (n = 15) and *Kcnq5*$^{dn/dn}$ (n = 16) mice. No statistical difference is observed between the two groups (P = 0.3, Student's t test). (*B*) (*Left* and *Center*) ImAHP in either *Kcnq5*$^{+/+}$ or *Kcnq5*$^{dn/dn}$ mice recorded from CA3 pyramidal neurons. (*Right*) Summary graph of the ImAHP amplitude in *Kcnq5*$^{+/+}$ (n = 21) and *Kcnq5*$^{dn/dn}$ (n = 13) mice. Asterisk indicates $P < 0.05$ (Student's t test). (*C*) (*Left* and *Center*) IsAHP in either *Kcnq5*$^{+/+}$ or *Kcnq5*$^{dn/dn}$ mice recorded from CA1 pyramidal neurons. (*Right*) Summary graph of the sAHP charge in *Kcnq5*$^{+/+}$ (n = 15) and *Kcnq5*$^{dn/dn}$ (n = 16) mice. No statistical difference is observed between the two groups (P = 0.74, Student's t test). (*D*) (*Left* and *Center*) IsAHP in either *Kcnq5*$^{+/+}$ or *Kcnq5*$^{dn/dn}$ mice recorded from CA3 pyramidal neurons. (*Right*) Summary graph of the sAHP charge in *Kcnq5*$^{+/+}$ (n = 21) and *Kcnq5*$^{dn/dn}$ (n = 14) mice. Asterisk indicates $P < 0.005$ (Student's t test).

our data show that KCNQ5 channels contribute both to the mAHP and sAHP currents in the hippocampus. Our work raises the exciting possibility that KCNQ channels in general participate in the IsAHP. Our current and previous work using KCNQ3- and KCNQ2-deficient mice suggests that different cell types in the brain rely on a different set of KCNQ subunits for the AHP currents. Therefore, different cell types might express specific complements of KCNQ subunits tailored to fit their function in the brain. Finally, the differential cell-specific contribution of individual KCNQ isoforms to neuronal K^+ currents is likely to underlie the different phenotypes of mice without functional KCNQ2, KCNQ3 (12, 14, 27, 43), and KCNQ5 channels (this work).

Materials and Methods

Generation of Kcnq5$^{dn/dn}$ Mice. A 129/SvJ genomic λ-phage library (Lambda FIX II Library; Stratagene) was screened with a *kcnq5* cDNA probe spanning the pore region. Inserts from hybridizing λ-clones were subcloned into the NotI site of the pKO901-DTA vector (Lexicon Genetics) and analyzed by PCR and Southern blotting for the presence of exon 6. A positive clone was identified and fully sequenced. A 6.6-kb BamHI/BstBI fragment was subcloned into the BamHI/ClaI sites of the pKO901-DTA vector, and a floxed NEO resistance cassette from pKO800 (Lexicon Genetics) was inserted in the BstEII site of intron 5. The dominant negative G278S point mutation was introduced into the WT pore motif by PCR-based mutagenesis. This change also included a silent BsiWI restriction site for easy genotyping, and the resulting construct was verified by sequencing. The vector was linearized with *Not*I and electroporated into MPI-2 mouse ES cells. ES cells surviving the G418 selection were screened for correct targeting by Southern blot analysis of EcoRV-digested DNA. ES cell clones having undergone homologous recombination were transfected with a plasmid expressing Cre-recombinase to remove the NEO cassette, thereby leaving a single loxP site. Cells were injected into C57BL/6 blastocysts, and highly chimeric mice were mated to produce the first filial generation.

Genotyping. Genotyping of KCNQ5 mice was performed by PCR using the following primer pair: 5′-acccataaattctccccaacatgatcacc-3′, 5′-attacttgtttgtttctagggttgaccgtttgg-3′. This resulted in a fragment of 231 bp for WT and 265 base pairs for the dominant negative allele.

Quantitative Real-Time RT-PCR. Total RNA was prepared from brains of WT and *Kcnq5*$^{dn/dn}$ mice using TRIZOL (Invitrogen), digested with RNase-free DNase (Ambion) and purified with RNeasy columns (Qiagen). cDNA synthesis used SuperScript II reverse transcriptase (Invitrogen), oligo(dT)$_{15}$ primer, first-strand reaction buffer, 0.1 M DTT, 10 mM dNTP mix, and RNaseOUT (Invitrogen). The quantitative RT-PCR assay was run on an ABI PRISM 7700 Sequence detection System (SDS 2.1 software) using SYBR green PCR master mix (Applied Biosystems). Primers used were 5′-gggcacaatcacactgacaacc-3′ and 5′-gaaagaaatgccaaggagtgcg-3′. For quantification, we used the $2^{-\Delta\Delta Ct}$ method, taking HPRT and GAPDH as reference genes.

Antibodies. Polyclonal antisera were raised in rabbits against peptides corresponding to amino acids 16–37 of KCNQ2 (GEKKLKVGFVGLDPGAPDSTRD), 858–873 of KCNQ3 (GDGISDSIWTPSNKPT), and 813–828 of KCNQ5 (SESSGSRGSQDFYPK). These peptides contained an additional carboxy terminal cysteine for coupling to a carrier protein (keyhole limpet hemocyanin). Antisera were affinity-purified against the corresponding peptide coupled to Sulfolink-Sepharose (Pierce) and tested by Western blotting (Fig. 1*F*) and immunocytochemistry (Fig. S3) of tsA or HeLa cells transiently transfected with the corresponding pcDNA3$^+$-KCNQ vector DNA. The ankyrin G antibody was from Zymed, and the antisynaptophysin antibody was from Synaptic Systems.

Western Blotting. Brain membrane proteins (50–100 μg per lane) were separated by SDS/PAGE (8.5%); blotted to PVDF membranes; and probed with affinity-purified anti-KCNQ2 (1:1,000), anti-KCNQ3 (1:200), anti-KCNQ5 (1:200), and antisynaptophysin (1:5,000) antibodies. Detection used ECL Western blotting substrate. Details are provided in *SI Materials and Methods*.

Histology. Nissl staining, immunostaining using DAB, and immunofluorescence analysis were performed on brain sections from perfusion-fixed mice, as detailed in *SI Materials and Methods*. Sections were examined with a Zeiss Axiophot or Zeiss Stemi-2000-c microscope or by confocal laser-scanning microscopy (LSM510; Zeiss) for immunofluorescence.

Expression in *Xenopus* Oocytes and Two-Electrode Voltage Clamping. *Xenopus* oocytes were obtained and injected as described elsewhere (15). A final amount of 20 ng of cRNA was injected per oocyte for each condition. Oocytes were incubated for 3–4 days at 17 °C and then examined by two-electrode voltage clamping using a Turbo Tec03 (NPI Electronics) amplifier and pClamp 8.0 software (Molecular Devices). The protocol consisted of 5-s steps from −110 to +50 mV in 10-mV increments from a holding potential of −80 mV.

Slice Electrophysiology. Transverse hippocampal slices (300 μm) were prepared from either 12- to 19-day-old WT or *Kcnq5*$^{dn/dn}$ mice. The ImAHP and IsAHP were determined following a 100-ms voltage step to +25 mV from a holding membrane potential of −55 mV. To determine the QsAHP, we integrated the sAHP current for 19 s starting 450 ms after the depolarizing voltage step. All recordings were made in the presence of 0.5 μM TTX (more details are provided in *SI Materials and Methods*).

ACKNOWLEDGMENTS. We thank Vitya Verdanyan for breeding *Kcnq5*^{dn} mice and testing antibodies and Patrick Seidler for technical assistance. This work was partially supported by grants from the European Union (Grant FP6, KCNQpathies) and the Leibniz Gesellschaft to T.J.J. R.A.N. and A.V.T. are supported by National Institutes of Health grants. G.S. is a fellow of the AvHumboldt Foundation.

1. Nicoll RA (1988) The coupling of neurotransmitter receptors to ion channels in the brain. *Science* 241:545–551.
2. Storm JF (1990) Potassium currents in hippocampal pyramidal cells. *Prog Brain Res* 83: 161–187.
3. Vogalis F, Storm JF, Lancaster B (2003) SK channels and the varieties of slow after-hyperpolarizations in neurons. *Eur J Neurosci* 18:3155–3166.
4. McCormick DA (1989) Cholinergic and noradrenergic modulation of thalamocortical processing. *Trends Neurosci* 12:215–221.
5. Fernández de Sevilla D, Garduño J, Galván E, Buño W (2006) Calcium-activated afterhyperpolarizations regulate synchronization and timing of epileptiform bursts in hippocampal CA3 pyramidal neurons. *J Neurophysiol* 96:3028–3041.
6. Sah P, Bekkers JM (1996) Apical dendritic location of slow afterhyperpolarization current in hippocampal pyramidal neurons: Implications for the integration of long-term potentiation. *J Neurosci* 16:4537–4542.
7. Oh MM, Kuo AG, Wu WW, Sametsky EA, Disterhoft JF (2003) Watermaze learning enhances excitability of CA1 pyramidal neurons. *J Neurophysiol* 90:2171–2179.
8. Disterhoft JF, Coulter DA, Alkon DL (1986) Conditioning-specific membrane changes of rabbit hippocampal neurons measured in vitro. *Proc Natl Acad Sci USA* 83: 2733–2737.
9. Tzingounis AV, Kobayashi M, Takamatsu K, Nicoll RA (2007) Hippocalcin gates the calcium activation of the slow afterhyperpolarization in hippocampal pyramidal cells. *Neuron* 53:487–493.
10. Burgoyne RD (2007) Neuronal calcium sensor proteins: Generating diversity in neuronal Ca2+ signalling. *Nat Rev Neurosci* 8:182–193.
11. Stocker M (2004) Ca(2+)-activated K+ channels: Molecular determinants and function of the SK family. *Nat Rev Neurosci* 5:758–770.
12. Tzingounis AV, Nicoll RA (2008) Contribution of KCNQ2 and KCNQ3 to the medium and slow afterhyperpolarization currents. *Proc Natl Acad Sci USA* 105:19974–19979.
13. Wang HS, et al. (1998) KCNQ2 and KCNQ3 potassium channel subunits: Molecular correlates of the M-channel. *Science* 282:1890–1893.
14. Peters HC, Hu H, Pongs O, Storm JF, Isbrandt D (2005) Conditional transgenic suppression of M channels in mouse brain reveals functions in neuronal excitability, resonance and behavior. *Nat Neurosci* 8:51–60.
15. Schroeder BC, Hechenberger M, Weinreich F, Kubisch C, Jentsch TJ (2000) KCNQ5, a novel potassium channel broadly expressed in brain, mediates M-type currents. *J Biol Chem* 275:24089–24095.
16. Lerche C, et al. (2000) Molecular cloning and functional expression of KCNQ5, a potassium channel subunit that may contribute to neuronal M-current diversity. *J Biol Chem* 275:22395–22400.
17. Jensen HS, Callø K, Jespersen T, Jensen BS, Olesen SP (2005) The KCNQ5 potassium channel from mouse: A broadly expressed M-current like potassium channel modulated by zinc, pH, and volume changes. *Brain Res Mol Brain Res* 139:52–62.
18. Kharkovets T, et al. (2000) KCNQ4, a K^+ channel mutated in a form of dominant deafness, is expressed in the inner ear and the central auditory pathway. *Proc Natl Acad Sci USA* 97:4333–4338.
19. Russell MW, Dick M, 2nd, Collins FS, Brody LC (1996) KVLQT1 mutations in three families with familial or sporadic long QT syndrome. *Hum Mol Genet* 5:1319–1324.
20. Kubisch C, et al. (1999) KCNQ4, a novel potassium channel expressed in sensory outer hair cells, is mutated in dominant deafness. *Cell* 96:437–446.
21. Schroeder BC, Kubisch C, Stein V, Jentsch TJ (1998) Moderate loss of function of cyclic-AMP-modulated KCNQ2/KCNQ3 K+ channels causes epilepsy. *Nature* 396:687–690.
22. Lein ES, et al. (2007) Genome-wide atlas of gene expression in the adult mouse brain. *Nature* 445:168–176.
23. Jentsch TJ (2000) Neuronal KCNQ potassium channels: Physiology and role in disease. *Nat Rev Neurosci* 1:21–30.
24. Brown DA, Passmore GM (2009) Neural KCNQ (Kv7) channels. *Br J Pharmacol* 156: 1185–1195.
25. Gu N, Vervaeke K, Hu H, Storm JF (2005) Kv7/KCNQ/M and HCN/h, but not KCa2/SK channels, contribute to the somatic medium after-hyperpolarization and excitability control in CA1 hippocampal pyramidal cells. *J Physiol* 566:689–715.
26. Wu WW, Chan CS, Surmeier DJ, Disterhoft JF (2008) Coupling of L-type Ca2+ channels to KV7/KCNQ channels creates a novel, activity-dependent, homeostatic intrinsic plasticity. *J Neurophysiol* 100:1897–1908.
27. Watanabe H, et al. (2000) Disruption of the epilepsy KCNQ2 gene results in neural hyperexcitability. *J Neurochem* 75:28–33.
28. Sah P (1995) Properties of channels mediating the apamin-insensitive afterhyperpolarization in vagal motoneurons. *J Neurophysiol* 74:1772–1776.
29. Miceli F, Cilio MR, Taglialatela M, Bezanilla F (2009) Gating currents from neuronal K(V)7.4 channels: General features and correlation with the ionic conductance. *Channels* 3:274–283.
30. Valiante TA, Abdul-Ghani MA, Carlen PL, Pennefather P (1997) Analysis of current fluctuations during after-hyperpolarization current in dentate granule neurones of the rat hippocampus. *J Physiol* 499:121–134.
31. Li Y, Gamper N, Shapiro MS (2004) Single-channel analysis of KCNQ K+ channels reveals the mechanism of augmentation by a cysteine-modifying reagent. *J Neurosci* 24:5079–5090.
32. Tatulian L, Brown DA (2003) Effect of the KCNQ potassium channel opener retigabine on single KCNQ2/3 channels expressed in CHO cells. *J Physiol* 549:57–63.
33. Schwake M, Pusch M, Kharkovets T, Jentsch TJ (2000) Surface expression and single channel properties of KCNQ2/KCNQ3, M-type K+ channels involved in epilepsy. *J Biol Chem* 275:13343–13348.
34. Delmas P, Brown DA (2005) Pathways modulating neural KCNQ/M (Kv7) potassium channels. *Nat Rev Neurosci* 6:850–862.
35. Madison DV, Nicoll RA (1982) Noradrenaline blocks accommodation of pyramidal cell discharge in the hippocampus. *Nature* 299:636–638.
36. Schnee ME, Brown BS (1998) Selectivity of linopirdine (DuP 996), a neurotransmitter release enhancer, in blocking voltage-dependent and calcium-activated potassium currents in hippocampal neurons. *J Pharmacol Exp Ther* 286:709–717.
37. Gerlach AC, Maylie J, Adelman JP (2004) Activation kinetics of the slow afterhyperpolarization in hippocampal CA1 neurons. *Pflugers Arch* 448:187–196.
38. Madison DV, Nicoll RA (1986) Cyclic adenosine 3′,5′-monophosphate mediates beta-receptor actions of noradrenaline in rat hippocampal pyramidal cells. *J Physiol* 372: 245–259.
39. Pedarzani P, Krause M, Haug T, Storm JF, Stühmer W (1998) Modulation of the Ca2+-activated K+ current sIAHP by a phosphatase-kinase balance under basal conditions in rat CA1 pyramidal neurons. *J Neurophysiol* 79:3252–3256.
40. Grabauskas G, Lancaster B, O'Connor V, Wheal HV (2007) Protein kinase signalling requirements for metabotropic action of kainate receptors in rat CA1 pyramidal neurones. *J Physiol* 579:363–373.
41. Alger BE, Nicoll RA (1980) Epileptiform burst afterhyperolarization: Calcium-dependent potassium potential in hippocampal CA1 pyramidal cells. *Science* 210: 1122–1124.
42. Hotson JR, Prince DA (1980) A calcium-activated hyperpolarization follows repetitive firing in hippocampal neurons. *J Neurophysiol* 43:409–419.
43. Singh NA, et al. (2008) Mouse models of human KCNQ2 and KCNQ3 mutations for benign familial neonatal convulsions show seizures and neuronal plasticity without synaptic reorganization. *J Physiol* 586:3405–3423.